REPORT DOCUMENTATION PAGE

Form Approved
OMB No. 0704-01-0188

PLEASE DO NOT RETURN YOUR FORM TO THE ABOVE ADDRESS.

1. REPORT DATE (DD-MM-YYYY)	2. REPORT TYPE	3. DATES COVERED (From - To)
01-12-2007	REPRINT	

4. TITLE AND SUBTITLE

Simple approximations of quasi-linear diffusion coefficients

5a. CONTRACT NUMBER

5b. GRANT NUMBER

5c. PROGRAM ELEMENT NUMBER
62601F

6. AUTHORS
J.M. Albert

5d. PROJECT NUMBER
1010

5e. TASK NUMBER
RR

5f. WORK UNIT NUMBER
A1

7. PERFORMING ORGANIZATION NAME(S) AND ADDRESS(ES)

Air Force Research Laboratory /RVBXR
29 Randolph Road
Hanscom AFB, MA 01731-3010

8. PERFORMING ORGANIZATION REPORT NUMBER
AFRL-RV-HA-TR-2008-1013

9. SPONSORING/MONITORING AGENCY NAME(S) AND ADDRESS(ES)

10. SPONSOR/MONITOR'S ACRONYM(S)
AFRL/RVBXR

11. SPONSOR/MONITOR'S REPORT NUMBER(S)

12. DISTRIBUTION/AVAILABILITY STATEMENT
Approved for Public Release; distribution unlimited.

13. SUPPLEMENTARY NOTES
Reprinted from *Journal of Geophysical Reseeach:* Vol. 112, A12202, doi:10.1029/2007JA012551, 2006

14. ABSTRACT

Quasi-linear diffusion by cyclotron-resonant plasma waves is likely a key ingredient of the behavior of electrons in the Earth's radiation belts. Multidimensional dynamical simulations are under development, which require the diffusion coefficients to be evaluated quickly as well as accurately. The recently developed parallel propagation approximation replaces the integration over wavenormal distribution to a closed form expression, and can be quite accurate. However, it can also perform badly, especially for electron energy ≥1 MeV. Here, the accuracy, justification, and limits of the approximation are explored, and an improved version is presented. It is based on a previously developed procedure for identifying wavenormal angles compatible with imposed cutoffs on the wave frequency distribution. Because it also requires evaluation at only a small number of points, it features computational efficiency comparable to the parallel propagation version, while preserving contributions from oblique waves and all relevant harmonic numbers. Detailed comparisons are presented using an established model of nightside chorus.

15. SUBJECT TERMS
Diffusion coefficients Radiation belts Quasilinear theory

16. SECURITY CLASSIFICATION OF:			17. LIMITATION OF ABSTRACT	18. NUMBER OF PAGES	19a. NAME OF RESPONSIBLE PERSON
a. REPORT	b. ABSTRACT	c. THIS PAGE			J. M. Albert
UNCL	UNCL	UNCL	UNL	10	19B. TELEPHONE NUMBER (Include area code)

JOURNAL OF GEOPHYSICAL RESEARCH, VOL. 112, A12202, doi:10.1029/2007JA012551, 2007

Simple approximations of quasi-linear diffusion coefficients

J. M. Albert[1]

Received 18 May 2007; revised 31 July 2007; accepted 10 September 2007; published 1 December 2007.

[1] Quasi-linear diffusion by cyclotron-resonant plasma waves is likely a key ingredient of the behavior of electrons in the Earth's radiation belts. Multidimensional dynamical simulations are under development, which require the diffusion coefficients to be evaluated quickly as well as accurately. The recently developed parallel propagation approximation replaces the integration over wavenormal distribution with a closed form expression, and can be quite accurate. However, it can also perform badly, especially for electron energy $\geq$1 MeV. Here, the accuracy, justification, and limits of the approximation are explored, and an improved version is presented. It is based on a previously developed procedure for identifying wavenormal angles compatible with imposed cutoffs on the wave frequency distribution. Because it also requires evaluation at only a small number of points, it features computational efficiency comparable to the parallel propagation version, while preserving contributions from oblique waves and all relevant harmonic numbers. Detailed comparisons are presented using an established model of nightside chorus.

Citation: Albert, J. M. (2007), Simple approximations of quasi-linear diffusion coefficients, *J. Geophys. Res.*, *112*, A12202, doi:10.1029/2007JA012551.

1. Introduction

[2] Quasi-linear diffusion by cyclotron-resonant plasma waves [*Horne and Thorne*, 1998] have been established as a likely key ingredient of the behavior of electrons in the Earth's radiation belts. In particular, attention has focused on whistler mode chorus [*Horne et al.*, 2005], hiss [*Meredith et al.*, 2006], and electromagnetic ion cyclotron (EMIC) waves [*Summers and Thorne*, 2003], alone and in combination [*Summers et al.*, 1998]. In conjunction with increasingly compelling empirical studies [e.g., *Meredith et al.*, 2003a, 2003b; *Iles et al.*, 2006], multidimensional diffusion simulations are being developed [*Albert and Young*, 2005; *Varotsou et al.*, 2005; *Shprits et al.*, 2006a]. Such simulations require diffusion coefficients evaluated for many values of energy, equatorial pitch angle α_0, and (in 3D) L value, under a wide variety of evolving geophysical conditions. Furthermore, the simulation of, say, 1 MeV electrons requires a computational domain (and diffusion coefficients) extending significantly beyond 1 MeV, where boundary conditions (usually $f = 0$) are applied. Thus the diffusion coefficients must be evaluated reasonably quickly, as well as reasonably accurately.

[3] Toward this end, *Summers* [2005, 2007a, 2007b] have developed the parallel propagation approximation, which collapses the usual broad wavenormal distribution of the waves to a magnetic field-aligned (or anti-aligned) population. The integration over wavenormal angle θ of quasi-linear theory, which picks the resonant waves out of the distribution, is replaced by a closed form expression which is, naturally, much faster and easier to evaluate. The neglect of oblique waves also removes contributions with resonant harmonic number n other than -1. Contrary to long-established expectations based on plasmaspheric hiss [*Lyons et al.*, 1972; *Albert*, 1994, 1999], preliminary comparison of this approach with full quasi-linear calculations [*Shprits et al.*, 2006b] indicated surprisingly good agreement, with one caveat discussed in section 2.4.

[4] This paper explores further the accuracy of the parallel propagation approximation, interprets it as a weighted average over wavenormal angle θ of the full expression, shows where it is likely to perform poorly, and suggests an improved version. This modification is based on previously developed procedures for identifying wavenormal angles compatible with frequency cutoffs imposed on the modeled wave distribution. It also replaces an integration over wavenormal angle with evaluation at a small number of values, while retaining contributions from oblique waves and relevant harmonic resonance numbers. The contribution from $n = -1$ is as good an approximation to the true value as the parallel propagation result is, while the additional terms estimate their counterparts in the full calculation. The result is a more favorable compromise between computational speed and qualitative accuracy. These features are demonstrated for several versions of calculations using an established model of nightside

[1]Air Force Research Laboratory, Space Vehicles Directorate, Hanscom Air Force Base, Massachusetts, USA.

chorus appropriate for L = 4.5, for a wide range of energy and equatorial pitch angle.

2. Diffusion Coefficients

[5] With slight change of notation from *Albert* [2005], the local pitch angle diffusion coefficient $D_{\alpha\alpha}$ of *Lyons* [1974b], with dimensions of p^2/t, can be written as

$$\frac{D_{\alpha\alpha}}{p^2} = \frac{\Omega_c}{\gamma^2}\frac{B^2_{\rm wave}}{B^2_o}\sum_{n=-\infty}^{\infty}\sum_{\omega} D^n_{\alpha\alpha},$$
$$D^n_{\alpha\alpha} = \int_{\theta_{\rm min}}^{\theta_{\rm max}} \sin\theta d\theta\, \Delta_n\, G_1 G_2, \tag{1}$$

with

$$\Delta_n(\omega,\theta) = \frac{\pi}{2}\frac{\sec\theta}{|v_\parallel/c|^3}\Phi_n^2\frac{\left(-\sin^2\alpha + sn\Omega_c/\omega\gamma\right)^2}{\left|1-\left(\partial\omega/\partial k_\parallel\right)_\theta/v_\parallel\right|}, \tag{2}$$

$$G_1(\omega) = \frac{\Omega_c B^2(\omega)}{\int_{\omega_{LC}}^{\omega_{UC}} B^2(\omega')d\omega'},\ G_2(\omega,\theta) = \frac{g_\omega(\theta)}{N(\omega)}, \tag{3}$$

$$N(\omega) = \int_{\theta_{\rm min}}^{\theta_{\rm max}} d\theta' \sin\theta' \Gamma g_\omega(\theta'),\quad \Gamma = \mu^2\left|\mu+\omega\frac{\partial\mu}{\partial\omega}\right|. \tag{4}$$

For $D_{\alpha p}$ (or D_{pp}), the only change is that $\Delta_n(\omega, \theta)$ is multiplied by one (or two) additional factors of $[\sin\alpha\cos\alpha/(-\sin^2\alpha + sn\Omega_c/\omega\gamma)]$.

[6] In these formulas μ is the refractive index, kc/ω, given as a function of (ω, θ) by cold plasma theory [e.g., *Stix*, 1992]. The term Φ_n^2 accounts for the relationships between the components of wave electric and magnetic fields as well as the gyroaveraging of the resonant wave-particle phase, and is given by equation (9) of *Lyons* [1974b]; it contains Bessel functions J_n and $J_{n\pm1}$ with argument $s\ k_\perp\ p_\perp/m\Omega_c$ (where s is the sign of the particle's charge, m is its rest mass, γ is its relativistic factor, and Ω_c is the absolute value of its nonrelativistic cyclotron frequency in the background magnetic field B_o). Mathematically, the Bessel functions are appreciable (and oscillatory) when the argument is $\geq|n|$. Since the argument can be written as $(s\omega\gamma/\Omega_c - n)\tan\alpha\tan\theta$, contributions from large $|n|$ are obviously favored by large θ, large energy, and resonant waves at the latitude of the mirror point (where α is maximum). In particular, Φ_n^2 and Δ_n are zero at $\theta = 0$ unless $n = -1$.

[7] The function $B^2(\omega)$ describes the frequency distribution of wave power, and is taken to be zero unless ω lies between the lower and upper cutoffs ω_{LC} and ω_{UC}. Similarly, the distribution of wave power with wavenormal angle θ is described by $g_\omega(\theta)$, which is zero unless θ lies between $\theta_{\rm min}$ and $\theta_{\rm max}$. It is standard, though not necessary, to use truncated Gaussian distributions: $B^2(\omega) = \exp[-(\omega - \omega_m)^2/\delta\omega^2]$ and $g_\omega(\theta) = \exp[-(\tan\theta - \tan\theta_m)^2/\tan^2(\delta\theta)]$. The effect of using a Gaussian in $\tan\theta$ instead of θ in the model is to reduce the power ascribed to large values of θ.

[8] In equation (1), $G_2(\omega, \theta)$ and $\Delta_n(\omega, \theta)$ are evaluated at the resonant frequency ω corresponding to θ and n, determined from the cyclotron resonance condition. There may be several such values of ω, hence the sum over ω in (1). Thus for each n, $\Delta_n(\omega, \theta)$ and $G_1(\omega)$ are just functions of θ. However, in evaluating $N(\omega)$, the function Γ is evaluated at $(\omega(\theta), \theta')$. The functional form of Γ arises from the Jacobian of a transformation from $(k_\perp, k_\parallel)$ to (ω, θ), as discussed in the Appendix of *Lyons* [1974b].

[9] The purpose of writing the diffusion coefficients in the form equation (1) is to try to isolate the dependence of $D^n_{\alpha\alpha}$ on the parameters of the frequency and wavenormal distributions. Thus Δ_n and Γ are independent of the modeled wavefield, G_1 depends only on the frequency parameters, and (for ω within the frequency cutoffs) G_2 and $N(\omega)$ depend only on the wavenormal parameters.

2.1. Resonances

[10] The resonance condition is usually given as

$$\omega - k_\parallel v_\parallel = sn\Omega_c/\gamma. \tag{5}$$

However, it is also usually assumed that the wave intensity is distributed symmetrically with respect to the sign of $k_\parallel$, so that the particle encounters equatorward and anti-equatorward waves at every instant [*Lyons et al.*, 1971]. This is automatically accounted for by solving

$$(\omega - sn\Omega_c/\gamma)^2 = \left(k_\parallel v_\parallel\right)^2. \tag{6}$$

rather than equation (5), for frequencies of resonant waves in either direction. These resonances all occur in 1/4 bounce, from the equator to the mirror point, without accounting for the sign of $k_\parallel v_\parallel$ [*Lyons et al.*, 1972]. Note that the integrals in equation (1) and equation (4) are only over positive values of θ, which might more properly be written as $|\theta|$. If, instead, the same total wave intensity is distributed among only anti-equatorward waves (as is probably more realistic for chorus and EMIC waves), the particle takes twice as long (going from equator to mirror point and back) to encounter resonances with either sign of $k_\parallel v_\parallel$. However, for the same total intensity $B^2_{\rm wave}$, each resonant wave will have twice the power as in the bidirectional case, so the bounce averaged result will be the same. The prescription for bounce averaging, while transforming from local α to equatorial α_0, was given by *Lyons et al.* [1972].

2.2. Behavior of the Terms

[11] The behavior of the various terms vs. θ is shown in Figures 1 and 2, for 1 MeV electrons with $\alpha = 60°$ and $\omega_{pe}/\Omega_e = 2.5$ (given this ratio, it is not necessary to specify the L value). The top panels show $\Delta_n(\omega, \theta)$ and also Φ_n^2. As illustrated for both $n = -1$ and $n = -2$, the Bessel function term Φ_n^2 tends to be the controlling factor of Δ_n.

[12] The middle panels show $\omega(\theta)$ and also $G_1(\omega)$. To calculate G_1, the frequency parameters were taken to be $\omega_m = 0.35\Omega_e$, $\delta\omega = 0.15\Omega_e$, $\omega_{LC} = 0.05\Omega_e$, and $\omega_{UC} = 0.65\Omega_e$, as in the nightside chorus model of *Horne et al.* [2003]. Note that the variation of ω with θ is suprisingly weak for small and moderate θ, and lies well within the frequency cutoffs. This may be rationalized by considering

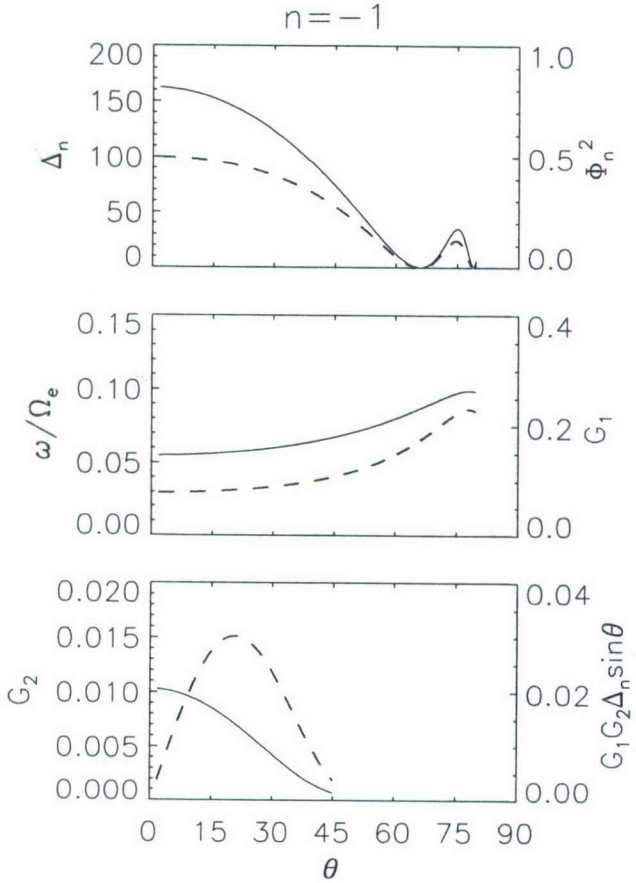

Figure 1. The behavior of various factors of the diffusion coefficients for 1 MeV electrons, with $\alpha = 60°$, $\omega_{pe}/\Omega_e = 2.5$ and $n = -1$. The various frequency and wavenormal parameters, for nightside chorus, are given in the text. Top panel: $\Delta_n(\omega, \theta)$ (left vertical axis) and Φ_n^2 (right vertical axis). Middle panel: $\omega(\theta)$ (left axis) and $G_1(\omega)$ (right axis). Bottom panel: G_2 (left axis) and $G_1G_2\,\Delta_n\,\sin\theta$ (right axis).

the resonance condition in the form $V(\omega, \theta) = \Psi(\omega, \theta)$, where $\Psi = \omega^2/k^2c^2$, as discussed in detail by *Albert* [2005]. Plotted against ω at fixed θ, the curves of V and Ψ both decrease as θ increases, so that the location of their intersection tends not to change much. From another point of view, the simplified treatment of *Lyons et al.* [1972] gave $\omega \sim \sec^2\theta$ (or $\omega \sim \cos^2\theta$ for $n = 0$), so that ω is nearly constant ($\partial\omega/\partial\theta$ is small) for small θ. This near constancy of $\omega(\theta)$ will be exploited in the next section.

[13] The bottom panels of Figures 1 and 2 show G_2 and the product $G_1G_2\Delta_n\,\sin\theta$, whose integral is $D^n_{\alpha\alpha}$. The wavenormal parameters $\theta_m = 0$, $\delta\theta = 30°$, $\theta_{\min} = 0$, $\theta_{\max} = 45°$ were used, also as done by *Horne et al.* [2003]. It is seen that the interplay between Φ_n and $G_2\,\sin\theta$ controls which θ values contribute to $D^n_{\alpha\alpha}$.

2.3. Interpretation as a θ Average

[14] As noted above, the middle panels of Figures 1 and 2 show that for small and moderate θ values $\omega(\theta)$ is roughly constant. Thus in evaluating the normalization $N(\omega)$, it may be acceptable to replace $\Gamma(\omega(\theta), \theta')$ with $\Gamma(\omega(\theta'), \theta')$. This approximation has the benefit that N can then be taken outside the θ integral in equation (1), giving

$$D^n_{\alpha\alpha} \approx \frac{\int_{\theta_{\min}}^{\theta_{\max}} d\theta \sin\theta \Delta_n G_1 g_\omega(\theta)}{\int_{\theta_{\min}}^{\theta_{\max}} d\theta \sin\theta \Gamma g_\omega(\theta)}. \tag{7}$$

This form may be interpreted as a weighted average:

$$D^n_{\alpha\alpha} \approx \left\langle \frac{\Delta_n G_1}{\Gamma} \right\rangle, \tag{8}$$

with

$$\langle f(\theta)\rangle \equiv \frac{\int_{\theta_{\min}}^{\theta_{\max}} d\theta \sin\theta \Gamma(\omega(\theta), \theta) g_\omega(\theta) f(\theta)}{\int_{\theta_{\min}}^{\theta_{\max}} d\theta \sin\theta \Gamma(\omega(\theta), \theta) g_\omega(\theta)}. \tag{9}$$

Figure 3 shows Δ_n G_1/Γ and the weighting function $\sin\theta$ $\Gamma g_\omega(\theta)$ corresponding to Figures 1 and 2. Note that for $n = -1$, Δ_n G_1/Γ is practically constant for small θ, while much of the θ dependence in equation (1) has been isolated in the weighting function. Thus the weighted average of the relatively constant factors is expected to be insensitive to the exact form of the weighting function, and to the θ range over which the average is performed. The actual values of the weighted average are indicated by

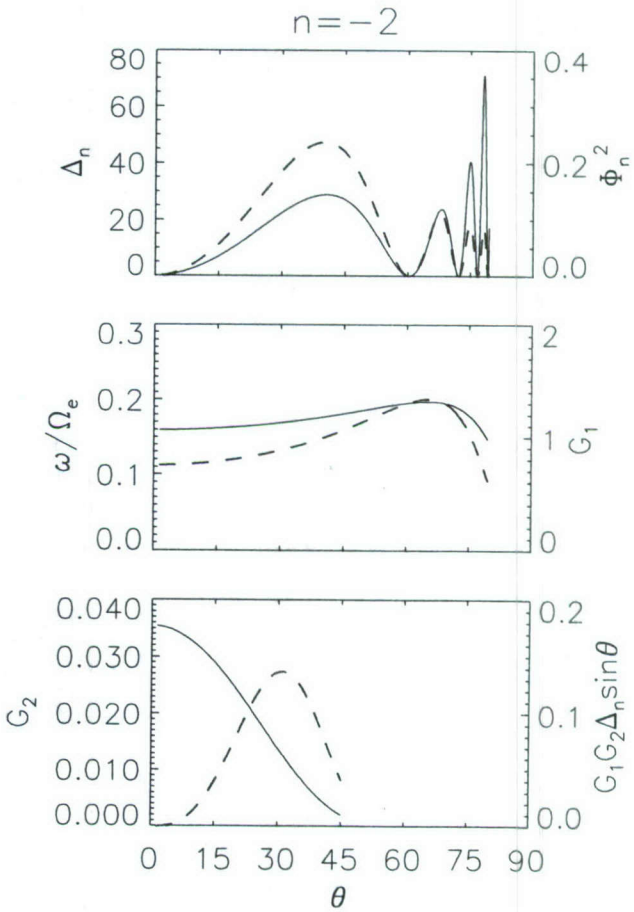

Figure 2. Same as Figure 1, for $n = -2$.

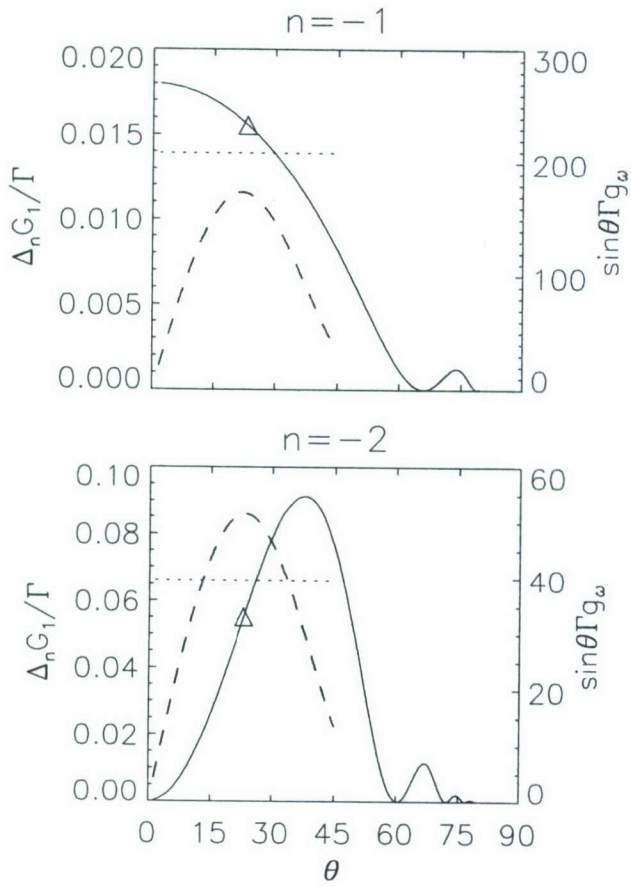

Figure 3. The combination $\Delta_n G_1/\Gamma$ and weighting function $\sin\theta\,\Gamma g_\omega(\theta)$ corresponding to Figures 1 and 2. The local diffusion coefficient $D_{\alpha\alpha}{}^n$ is approximated by the integral over θ of their product in equation (8). The weighted average of $\Delta_n G_1/\Gamma$ is indicated by the dotted curves, and its value evaluated at θ_r is shown by the triangles.

the dotted lines, while the points marked by triangles will be discussed below.

2.4. Evaluation at Discrete θ Values

[15] The well-known mean value theorem [e.g., *Gradshteyn and Ryzhik*, 1980] guarantees that the average of the expression in equation (8) can be obtained by simply evaluating it at a single (unknown) value θ_0 between $\theta_{\min}$ and $\theta_{\max}$:

$$D^n_{\alpha\alpha} \approx \frac{\Delta_n G_1}{\Gamma}\Big|_{\theta_0}. \tag{10}$$

With $\theta_0 = 0$, this result and the corresponding ones for $D^n_{\alpha p}$ and D^n_{pp} are exactly 1/2 times those of equations (5–7) of *Summers et al.* [2007a].

[16] Full numerical integration with the PADIE code [*Glauert and Horne*, 2005] also manifested this numerical factor relative to Summers [R. Horne, personal communication, 2006], which is evident, though not noted, in the plots of *Shprits et al.* [2006b]. The descrepancy is tentatively ascribed to the explicit factor of 2 in equation 1 of *Summers* [2005], which is not apparent in earlier work [*Kennel and Engelmann*, 1966, equation 4.1; *Lerche*, 1968, equation 14; *Lyons et al.*, 1971, equation 1; *Lyons*, 1974a, equation 1], and not to any error in the ensuing derivation. Pending the ultimate resolution of this issue, this paper will consider the parallel propagation approximation in the form of equation (10), with $\theta_0 = 0$.

[17] More generally, if equation (10) is to be a reasonable approximation to equation (8), the condition $\omega_{LC} < \omega(\theta_0) < \omega_{UC}$ is required; values of $\omega(\theta)$ which satisfy the resonance condition but do not lie within the cutoffs are termed noncontributing. Techniques for identifying such values of θ have previously been developed for whistler mode waves [*Albert*, 1999, 2004, 2005], EMIC waves [*Albert*, 2003], and superluminous and Z mode waves [*Albert*, 2007], for the purpose of performing the full integral equation (1) efficiently, and are reviewed in Appendix A. These techniques yield θ intervals, or ranges, (θ_a, θ_b), which can be directly applied to choosing where to estimate equation (8).

[18] If there is only one θ range, θ_0 is taken as some representative value such as $(\theta_a + \theta_b)/2$ or $\tan^{-1}[(\tan\theta_a + \tan\theta_b)/2]$ (as used below for convenience). If there is more than one θ range, (7–9) are expressed as sums of averages over each range r:

$$\begin{aligned} D^n_{\alpha\alpha} &\approx \sum\nolimits_r a_r \frac{\int_r d\theta \sin\theta \Delta_n G_1 g_\omega(\theta)}{\int_r d\theta \sin\theta \Gamma g_\omega(\theta)} \\ &\approx \sum\nolimits_r a_r \left\langle \frac{\Delta_n G_1}{\Gamma} \right\rangle_r \approx \sum_r a_r \frac{\Delta_n G_1}{\Gamma}\Big|_{\theta_r}, \end{aligned} \tag{11}$$

where

$$a_r \equiv \frac{\int_r d\theta \sin\theta \Gamma g_\omega(\theta)}{\sum_r \int_r d\theta \sin\theta \Gamma g_\omega(\theta)} \approx \frac{\int_r d\theta \sin\theta g_\omega(\theta)}{\sum_r \int_r d\theta \sin\theta g_\omega(\theta)}. \tag{12}$$

This few-point estimate captures at least some measure of the contribution to equation (1) by oblique waves and all n values. In favorable situations the θ ranges will be narrow, so that $\Delta_n G_1/\Gamma$ is nearly constant within each one; at worst, the procedure defaults to $\theta_r = (\theta_{\min} + \theta_{\max})/2$. Since each range may contain some noncontributing values as well as all contributing values, it is possible for the chosen θ_r to misrepresent an entire range as noncontributing; however, the techniques discussed in Appendix A are discriminating enough that this is rare. In Figure 3, the values of $\Delta_n G_1/\Gamma$ evaluated at θ_r are marked by triangles and give good approximations to the weighted averages, indicated by the dotted lines.

[19] The fractions a_r in equation (12) may be evaluated numerically. However, with $g_\omega(\theta)$ given by the truncated gaussian of $x = \tan\theta$ mentioned above, it is convenient to further approximate $\sin\theta\, d\theta = x dx/(1 + x^2)^{3/2}$ by simply $x dx$. For $x < 1$ this does little harm, as shown in Figure 4, and allows a_r to be evaluated analytically. This procedure was followed in the numerical evaluations below.

3. Results

[20] Figure 5 shows several versions of bounce-averaged diffusion coefficients calculated with $\omega_{pe}/\Omega_e = 2.5$, $\omega_M = 0.35\Omega_e$, $\delta\omega = 0.15\Omega_e$, $\omega_{LC} = 0.05\Omega_e$, $\Omega_{UC} = 0.65\Omega_e$, $\theta_m = 0$,

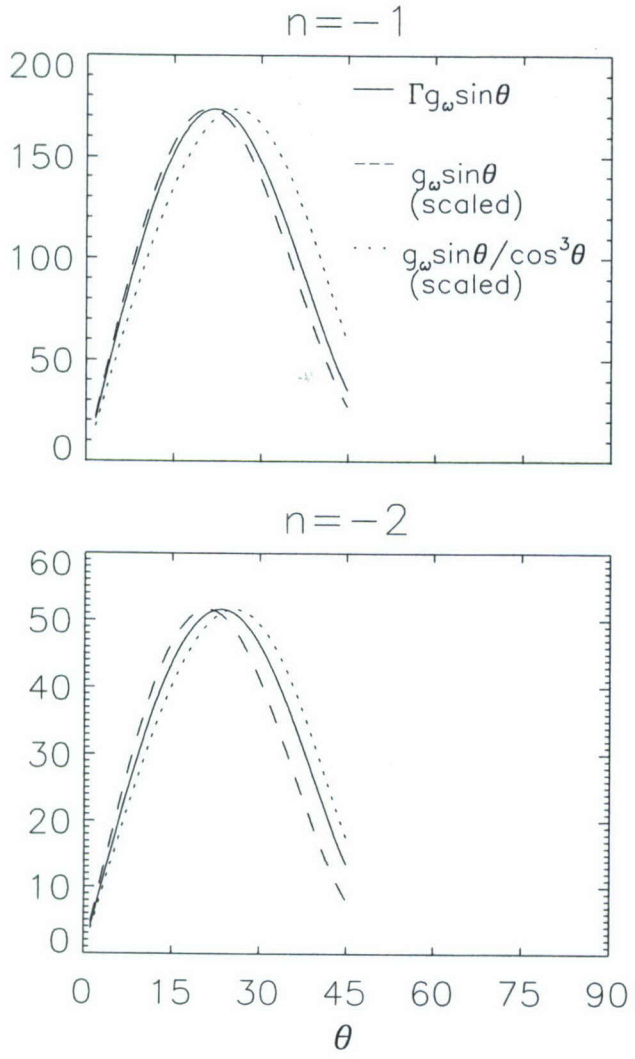

Figure 4. The weighting function $\sin\theta\,\Gamma g_\omega(\theta)$ of Figure 3 (solid curve), and the approximations $\sin\theta g_\omega(\theta)$ (dashed curve) and $\sin\theta g_\omega(\theta)/\cos^3\theta$ (dotted curve), where $g_\omega(\theta)$ is a Gaussian function of $\tan\theta$. The two approximations have been scaled to have the same maximum as the exact expression; the scale factor cancels in equation (12). The second approximation allows (12) to be evaluated analytically.

$\delta\theta = 30°$, $\theta_{min} = 0$, $\theta_{max} = 45°$ as above, $B_{wave} = 50$ pT, and latitude range $0 \le \lambda \le 15°$ [*Horne et al.*, 2005]. The black curves show the full calculation of equation (1), including all n between -5 and 5, which will be regarded as "the right answer," to be approximated.

[21] The green curves show equation (1) calculated with just $n = -1$, and are very close to the full results for 0.3 MeV, but miss dominant contributions from other n values for 1 MeV and especially 3 MeV below $\alpha_0 = 60°$. The red curves show equation (10) evaluated at $\theta_0 = 0$ (hence $n = -1$ only), as in *Shprits et al.* [2006b], while the blue curves show equation (11) evaluated with $\tan\theta_r$ at the center of the computed θ ranges, but only for $n = -1$. They (red and blue) are always close to each other and very close to the full results (black) for 0.3 MeV, but are only fair approximations to the full result for $n = -1$ (green) for higher energy and α_0 above 60°, and poor approximations to the full results. Finally, the magenta curve shows equation (11) again evaluated at θ_r but summed over $n = -5$ to 5, which seems to provide a good approximation to the full results (black).

[22] Figure 6 shows the same four approximations, normalized by the full calculation. Again, the green curves show equation (1) with $n = -1$ only, the red curves show equation (10) with $\theta_0 = 0$, and the blue curves show equation (11) with values of θ_r but $n = -1$ only. The magenta curve, showing equation (11) with the calculated values of θ_r and $n = -5$ to 5, clearly gives the best approximation (to a ratio of 1, shown by the dashed black line), with the exception of the region $\alpha_0 > 75°$, $E = 1$ MeV. Note that the region of good agreement in D_{pp} for the red curve at 1 MeV and 3 MeV between $\alpha_0 = 60°$ and 75° is

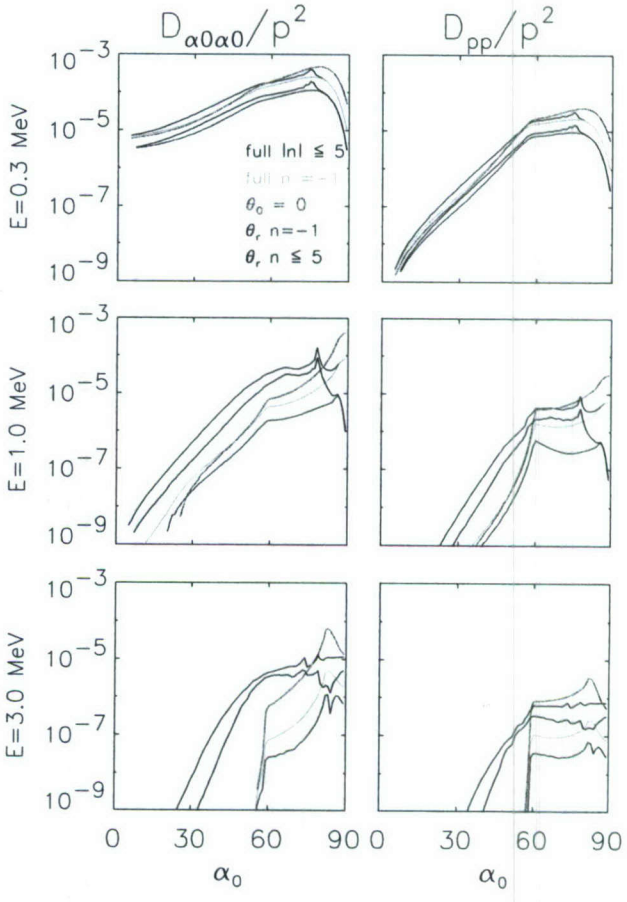

Figure 5. Several versions of bounce-averaged diffusion coefficients (in sec^{-1}) for 0.3 MeV, 1 MeV, and 3 MeV electrons and nightside chorus, with wave parameters given in the text. The black curves show the full calculation with $n \le 5$. The green curves show the full calculation with just $n = -1$. The red curves show results using the parallel propagation approximation. The blue curves show the "θ range" approximation discussed in the text, but only with $n = -1$. The magenta curves show the "θ range" approximation with $n \le 5$.

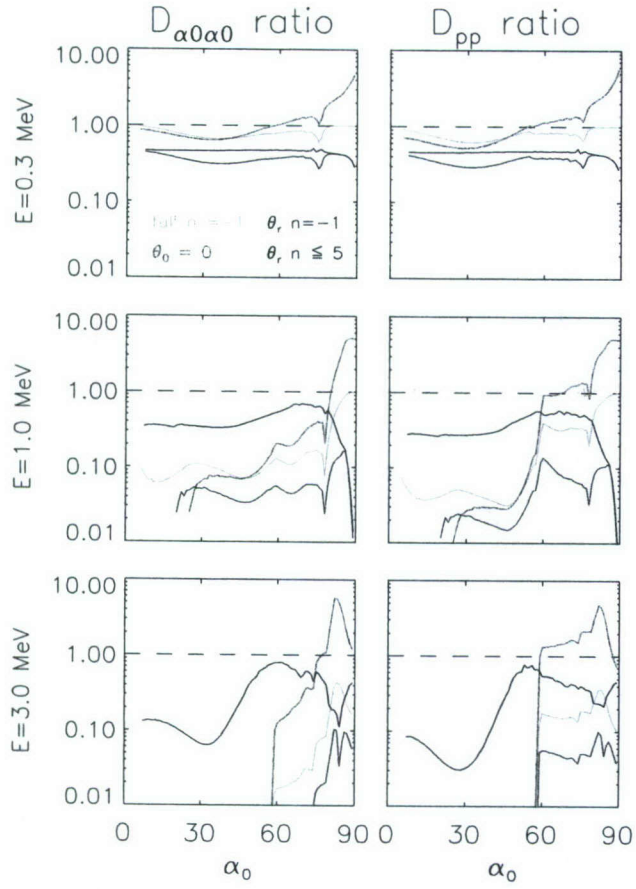

Figure 6. The four approximations shown in Figure 5, normalized by the results of the full calculation.

fortuitous because the green curve, computed from equation (1) with $n = -1$ only, also differs greatly, so that the diffusion actually comes from other n values, which the red (and blue) curves do not include. Also, the corresponding agreement in $D_{\alpha_0\alpha_0}$ is poor for all but the magenta curve.

3.1. Sensitivity to Parameter Changes

[23] Following *Shprits et al.* [2006b], Figure 7 shows the result of doubling the density ratio from $\omega_{pe}/\Omega_e = 2.5$ (solid curves) to 5.0 (dashed curves). The full calculations for 1 MeV, shown in black, show that the diffusion coefficients decrease at every α_0. The calculations using θ_r (blue) decrease as well, maintaining the same, mostly good, degree of approximation. The calculations using $\theta_0 = 0$ (red), which were only fair to begin with, become worse at the higher density.

[24] Figure 8 shows the effect of increasing the latitudinal extent of the waves, from 15° (solid curves) to 25° (dashed curves). None of the calculations are affected for $\alpha_0 \geq 60°$, since these particles mirror below 15° latitude. For smaller α_0, the calculations with $\theta_0 = 0$ (red) improve their agreement with the full calculations (black), but the calculations using θ_r (blue) improve even more, becoming almost indistinguishable from the full results with the wider latitude range.

[25] *Shprits et al.* [2006b] computed diffusion coefficients for different parameter values with $\theta_0 = 0$ and compared them to each other, and suggested that the variation of the results with the (imperfectly known) parameter values outweighed the benefit of performing the full calculations. However, this is not conclusive, because comparison was not made to full calculations using the same parameter values. The present results show that the parallel propagation approximation results are significantly more sensitive to the parameter changes than the full results are, while the approximations based on the θ ranges reproduce the behavior of the full calculations with good fidelity.

3.2. Qualitative Comparison at L = 4.5

[26] Figures 9–11 show diffusion coefficients calculated with the same wave model but with $\omega_{pe}/\Omega_e = 3.43$ on the

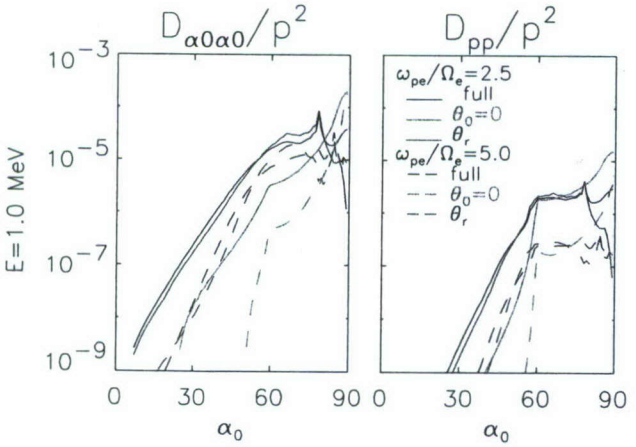

Figure 7. The effect of doubling the density ratio, from $\omega_{pe}/\Omega_e = 2.5$ (solid curves) to 5.0 (dashed curves), on diffusion rates (in sec^{-1}) for 1 MeV electrons. The full calculations are shown in black, the parallel propagation approximation in red, and the "θ range" approximation in blue.

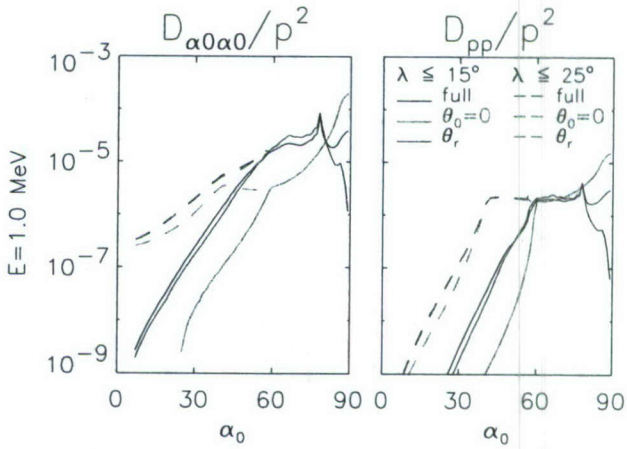

Figure 8. The effect of increasing the maximum latitudinal extent of nightside chorus from 15° (solid curves) to 25° (dashed curves). The full calculations are shown in black, the parallel propagation approximation in red, and the "θ range" approximation in blue. (The blue and black dashed curves are virtually indistinguishable.)

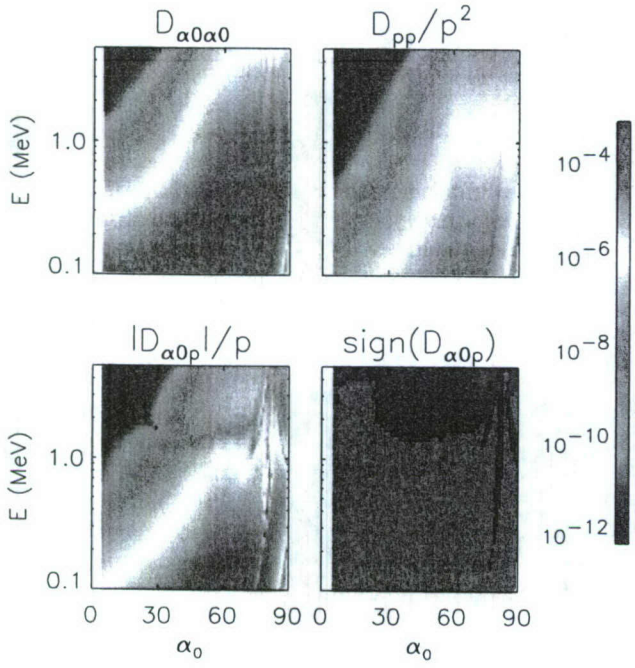

Figure 9. Diffusion coefficients (in s^{-1}) for electrons and nightside chorus waves with $\omega_{pe}/\Omega_e = 3.43$, for $E = 0.1$ MeV to 5 MeV, from a full calculation with $n \leq 5$.

equator, as appropriate for $L = 4.5$ [*Horne et al.*, 2005]. The calculations were done for 85 values of α_0 from 5° (just outside the loss cone) to 89°, and 49 logarithmically spaced values of energy between 0.1 MeV and 5 MeV (inclusive). Figure 9 shows the full calculations with n between −5 and 5, which took about 5 hours of computer time. Dark blue regions at the upper left corner (large E, small α_0) of panels (a), (b), and (c) are off the color scale, but are not zero. Figure 10 shows the results using the approximation equation (10) with at $\theta_0 = 0$ (and, necessarily, $n = -1$ only). They took only about 4 seconds to obtain, and show broad areas of qualitative agreement with Figure 9, but also show large areas of disagreement. The uncolored areas in the upper left of all four panels indicate diffusion coefficients of identically zero, indicating that no ($n = -1$) resonances were present. These regions include, but extend beyond, the dark blue small-value regions of Figure 9. Also, the cross diffusion coefficient is often estimated poorly, in that the boundary separating positive from negative values does not match Figure 10 at all well. Finally, Figure 11 shows the results using equation (11) using θ_r, for $n = -5$ to 5. These calculations took about 90 seconds, and show much better agreement with Figure 9 than Figure 10 does. Finite values are reported at all values of (E, α_0), and the general behavior of $D_{\alpha_0 p}$ is captured well.

4. Conclusions

[27] The local quasi-linear diffusion coefficients have been approximated as weighted averages over wavenormal angle θ. This relies on the resonant frequency ω being nearly constant as a function of wavenormal angle θ. Naturally, this is favored when θ_{max} is close to θ_{min} (so θ_{max} should be small if θ_{min} is small).

[28] Using previously developed techniques, the subranges of θ which contribute to the diffusion can be identified (see Appendix A), and the averages over each range can be further approximated by evaluation of equation (11) at single values θ_r. This retains the effect of oblique waves, and their resonances with arbitrary harmonic number n. The parallel propagation formulas [*Summers*,

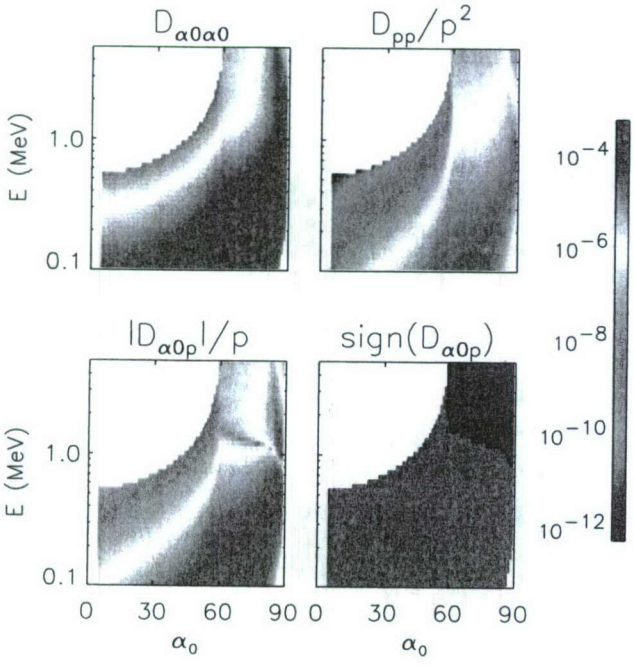

Figure 10. Same as Figure 9, but using the parallel propagation approximation.

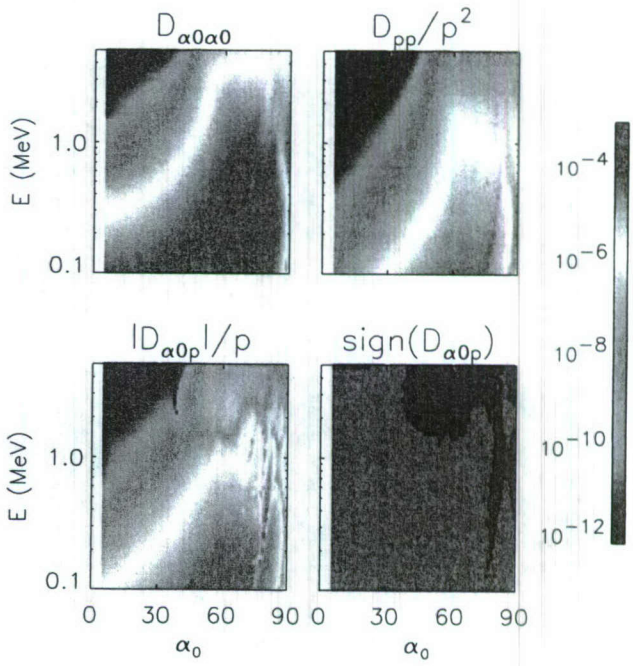

Figure 11. Same as Figure 9, but using the "θ range" approximation with $n \leq 5$.

2005, 2007a] are recovered by evaluation at $\theta = 0$ (hence $n = -1$ only), except for a factor of 2 as discussed. This approach may also be applied to EMIC waves [*Albert*, 2003] as well as to superluminous (L-X, L-O, and R-X) and Z mode waves which can be quite oblique [*Summers et al.*, 2001; *Albert*, 2007], though this is deferred to future work.

[29] The full integration of equation (1), as in *Albert* [2005] or *Horne et al.* [2005], remains the "gold standard" for such calculations, though they are moderately demanding of computer time. The parallel propagation expressions are much faster and easier to evaluate, and for typical chorus wave parameters give reasonable estimates of the $n = -1$ contribution, when present. However, this is not always the dominant term, especially for $E \geq 1$ MeV. The scheme presented here may be considered a hybrid of the approaches of *Summers* [2005] and *Albert* [2005]. It retains much of the convenience and most of the speed of the parallel propagation approximation with greater accuracy, as demonstrated for $\geq$1 MeV electrons interacting with chorus. Thus it may be an optimal approach for practical but comprehensive simulation of quasilinear diffusion in the radiation belts.

Appendix A: Finding Resonant θ Ranges

[30] To find conditions for resonant θ ranges consistent with lower and upper frequency cutoffs, the resonance condition equation (6) is written in some form $f(\omega, \theta) = g(\omega, \theta)$, and graphs of f and g are analyzed geometrically as functions of ω at fixed θ. Within the interval $(\omega_{LC}, \omega_{UC})$, the curves of $f(\omega)$ and $g(\omega)$ cannot intersect unless (i) $\max(f) > \min(g)$ (otherwise f always lies below g), and (ii) $\min(f) < \max(g)$ (otherwise f always lies above g). Imposing conditions (i) and (ii) retains all θ values for which $\omega(\theta)$ lies within the frequency cutoffs, while eliminating many though not necessarily all other θ values. Of course, the θ values are also required to lie between $\theta_{\min}$ and $\theta_{\max}$.

[31] The analysis has previously been performed for the resonance condition in the form

$$\frac{\omega^2}{k^2c^2} = \frac{v_\parallel^2}{c^2}\frac{\omega^2}{(\omega - \omega_n)^2}\cos^2\theta, \quad \omega_n \equiv sn\Omega_c/\gamma \tag{A1}$$

[*Albert*, 1999, 2003, 2005, 2007], because of the relatively simple geometric behavior of these expressions as functions of ω. The resonance condition can also be written as

$$k^2(\omega, \theta) = (\omega - \omega_n)^2\frac{\sec^2\theta}{v_\parallel^2} \equiv W(\omega, \theta). \tag{A2}$$

This form is even more convenient because k^2 is a monotonically increasing function of ω at fixed θ, for all cold plasma wave modes, while $W(\omega)$ also has simple behavior [*Albert*, 2007]. Thus for $\omega_n \leq 0$, condition (i) above becomes $k^2(\omega_{UC}) > W(\omega_{LC})$, while condition (ii) becomes $k^2(\omega_{LC}) < (\omega_{UC})$. For $\omega_n > 0$, there are three subcases. When $\omega_n < \omega_{LC}$, the conditions are the same as just given. When $\omega_n > \omega_{UC}$, the conditions become $k^2(\omega_{UC}) > W(\omega_{UC})$ and $k^2(\omega_{LC}) < W(\omega_{LC})$. Finally, when $\omega_{LC} < \omega_n < \omega_{UC}$, ω_{UC}, condition (i) is automatically satisfied since $\min(W) = 0$, while condition (ii) requires either $k^2(\omega_{LC}) < W(\omega_{LC})$ or $k^2(\omega_{LC}) < W(\omega_{UC})$. Each of these inequalities is easily converted to quadratic form, schematically

$$A\cos^4\theta + B\cos^2\theta + C > 0 \tag{A3}$$

(where the coefficients depend on ω_{LC} and ω_{UC}), so that θ ranges of the form $\theta_a \leq \theta \leq \theta_b$ are easily calculated from the roots of the quadratic. Limited numerical experiments indicate that these conditions based on (A2) are about as effective as corresponding conditions based on (A1), while being simpler to implement. Since they are not equivalent, both may be used.

[32] **Acknowledgments.** This work was supported by the Space Vehicles Directorate of the Air Force Research Laboratory.

[33] Zuyin Pu thanks Fuliang Xiao and another reviewer for their assistance in evaluating this paper.

References

Albert, J. M. (1994), Quasi-linear pitch-angle diffusion coefficients: Retaining high harmonics, *J. Geophys. Res.*, *99*, 23,741.

Albert, J. M. (1999), Analysis of quasi-linear diffusion coefficients, *J. Geophys. Res.*, *104*(A2), 2429.

Albert, J. M. (2003), Evaluation of quasi-linear diffusion coefficients for EMIC waves in a multi-species plasma, *J. Geophys. Res.*, *108*(A6), 1249, doi:10.1029/2002JA009792.

Albert, J. M. (2004), Analytical bounds on the whistler mode refractive index, *Phys. Plasmas*, *11*, 4875, doi:10.1063/1.1792634.

Albert, J. M. (2005), Evaluation of quasi-linear diffusion coefficients for whistler mode waves in a plasma with arbitrary density ratio, *J. Geophys. Res.*, *110*, A03218, doi:10.1029/2004JA010844.

Albert, J. M. (2007), Refractive index and wavenumber properties for cyclotron resonant quasilinear diffusion by cold plasma waves, *Phys. Plasmas*, *14*, 072901, doi:10.1063/1.2744363.

Albert, J. M., and S. L. Young (2005), Multidimensional quasi-linear diffusion of radiation belt electrons, *Geophys. Res. Lett.*, *32*, L14110, doi:10.1029/2005GL023191.

Glauert, S. A., and R. B. Horne (2005), Calculation of pitch angle and energy diffusion coefficients with the PADIE code, *J. Geophys. Res.*, *110*, A04206, doi:10.1029/2004JA010851.

Gradshteyn, I. S., and I. M. Ryzhik (1980), *Table of Integrals, Series, and Products*, Academic Press, New York.

Horne, R. B., and R. M. Thorne (1998), Potential waves for relativistic electron scattering and stochastic acceleration during magnetic storms, *Geophys. Res. Lett.*, *25*(15), 3011.

Horne, R. B., S. A. Glauert, and R. M. Thorne (2003), Resonant diffusion of radiation belt electrons by whistler-mode chorus, *Geophys. Res. Lett.*, *30*(9), 1493, doi:10.1029/2003GL016963.

Horne, B., R. M. Thorne, S. A. Glauert, J. M. Albert, N. P. Meredith, and R. R. Anderson (2005), Timescale for radiation belt electron acceleration by whistler mode chorus waves, *J. Geophys. Res.*, *110*, A03225, doi:10.1029/2004JA010811.

Iles, R. H. A., N. P. Meredith, A. N. Fazakerley, and R. B. Horne (2006), Phase space density analysis of the outer radiation belt energetic electron dynamics, *J. Geophys. Res.*, *111*, A03204, doi:10.1029/2005JA011206.

Kennel, C. F., and F. Engelmann (1966), Velocity space diffusion from weak plasma turbulence in a magnetic field, *Phys. Fluids*, *9*, 2377.

Lerche, I. (1968), Quasilinear theory of resonant diffusion in a magneto-active, relativistic plasma, *Phys. Fluids*, *11*, 1720.

Lyons, L. R. (1974a), General relations for resonant particle diffusion in pitch angle and energy, *J. Plasma Phys.*, *12*, 45.

Lyons, L. R. (1974b), Pitch angle and energy diffusion coefficients from resonant interactions with ion-cyclotron and whistler waves, *J. Plasma Phys.*, *12*, 417.

Lyons, L. R., R. M. Thorne, and C. F. Kennel (1971), Electron pitch angle diffusion driven by oblique whistler-mode turbulence, *J. Plasma Phys.*, *6*, 589.

Lyons, L. R., R. M. Thorne, and C. F. Kennel (1972), Pitch-angle diffusion of radiation belt electrons within the plasmasphere, *J. Geophys. Res.*, *77*, 3455.

Meredith, N. P., M. Cain, R. B. Horne, R. M. Thorne, D. Summers, and R. R. Anderson (2003a), Evidence for chorus-driven electron acceleration to relativistic energies from a survey of geomagnetically disturbed periods, *J. Geophys. Res.*, *108*(A6), 1248, doi:10.1029/2002JA009764.

Meredith, N. P., R. M. Thorne, R. B. Horne, D. Summers, B. J. Fraser, and R. R. Anderson (2003b), Statistical analysis of relativistic electron energies for cyclotron resonance with EMIC waves observed on CRRES, *J. Geophys. Res.*, *108*(A6), 1250, doi:10.1029/2002JA009700.

Meredith, N. P., R. B. Horne, S. A. Glauert, R. M. Thorne, D. Summers, J. M. Albert, and R. R. Anderson (2006), Energetic outer zone electron loss timescales during low geomagnetic activity, *J. Geophys. Res.*, *111*, A05212, doi:10.1029/2005JA011516.

Shprits, Y. Y., R. M. Thorne, R. B. Horne, S. A. Glauert, M. Cartwright, C. T. Russell, D. N. Baker, and S. G. Kanekal (2006a), Acceleration mechanism responsible for the formation of the new radiation belt during the 2003 Halloween solar storm, *Geophys. Res. Lett.*, *33*, L05104, doi:10.1029/2005GL024256.

Shprits, Y. Y., R. M. Thorne, R. B. Horne, and D. Summers (2006b), Bounce-averaged diffusion coefficients for field-aligned chorus, *J. Geophys. Res.*, *111*, A10255, doi:10.1029/2006JA011725.

Stix, T. H. (1992), *Waves in Plasmas*, American Institute of Physics, New York.

Summers, D. (2005), Quasi-linear diffusion coefficients for field-aligned electromagnetic waves with applications to the magnetosphere, *J. Geophys. Res.*, *110*, A08213, doi:10.1029/2005JA011159.

Summers, D., and R. M. Thorne (2003), Relativistic electron pitch-angle scattering by electromagnetic ion cyclotron waves during geomagnetic storms, *J. Geophys. Res.*, *108*(A4), 1143, doi:10.1029/2002JA009489.

Summers, D., R. M. Thorne, and F. Xiao (1998), Relativistic theory of wave-particle resonant diffusion with application to electron acceleration in the magnetosphere, *J. Geophys. Res.*, *103*, 20,487.

Summers, D., R. M. Thorne, and F. Xiao (2001), Gyroresonant acceleration of electrons in the magnetosphere by superluminous electromagnetic waves, *J. Geophys. Res.*, *106*(A6), 10,853.

Summers, D., B. Ni, and N. P. Meredith (2007a), Timescales for radiation belt electron acceleration and loss due to resonant wave-particle interactions: 1. Theory, *J. Geophys. Res.*, *112*, A04206, doi:10.1029/2006JA011801.

Summers, D., B. Ni, and N. P. Meredith (2007b), Timescales for radiation belt electron acceleration and loss due to resonant wave-particle interactions: 2. Evaluation for VLF chorus, ELF hiss, and electromagnetic ion cyclotron waves, *J. Geophys. Res.*, *112*, A04207, doi:10.1029/2006JA011993.

Varotsou, A., D. Boscher, S. Bourdarie, R. B. Horne, S. A. Glauert, and N. P. Meredith (2005), Simulation of the outer radiation belt electrons near geosynchronous orbit including both radial diffusion and resonant interaction with whistler-mode chorus waves, *Geophys. Res. Lett.*, *32*, L19106, doi:10.1029/2005GL023282.

J. M. Albert, Air Force Research Laboratory/VSBX, 29 Randolph Road, Hanscom AFB, MA 01731-3010, USA. (jay.albert@hanscom.af.mil)